Jurnal Teknologi

Full Paper

THE ANALYSIS OF PHASE, DISPERSION AND GROUP DELAY IN INGAASP/INP MICRORING RESONATOR

IS Amiri[a], SE Alavi[b], ASM Supa'at[b], J. Ali[c], H Ahmad[a]

[a]Photonics Research Centre, University of Malaya, 50603 Kuala Lumpur, Malaysia
[b]Faculty of Electrical Engineering, Universiti Teknologi Malaysia, 81310 UTM Johor Bahru Malaysia
[c]Laser Center, Ibnu Sina ISIR, Universiti Teknologi Malaysia, 81310 UTM Johor Bahru, Johor, Malaysia

*Corresponding author
abus@utm.my

Article history
Received
15 August 2015
Received in revised form
15 November 2015
Accepted
30 December 2015

Graphical abstract

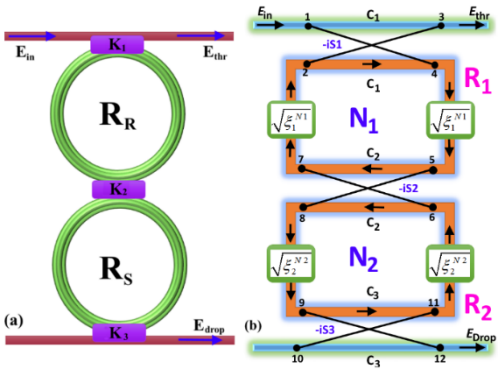

Abstract

The Vernier operation with signal flow graph (SFG) is a graphical approach for analyzing the intricate photonic circuits mathematically and quick calculation of optical transfer function. Analysis of a cascaded microring resonators (CMRR) made of InGaAsP/InP semiconductor is presented using the signal flow graph (SFG) method which enables modelling the transfer function of the passive CMRR. These passive filters are mostly characterized by their frequency response. The theoretical calculations of the system is performed by the Vernier effects analysis. Two MRRs with radius of 100 µm which are vertically coupled together are used to generate resonant peaks. Here, the phase, dispersion and group delay of the generated signals are analyzed.

Keywords: InGaAsP/InP semiconductor, cascaded microring resonators (CMRR), Vernier effects, phase, dispersion and group delay

Abstrak

Operasi Vernier dengan graf aliran isyarat (SFG) adalah satu pendekatan grafik untuk menganalisis litar fotonik rumit matematik dan pengiraan cepat fungsi pemindahan optik. Analisis resonator microring yang disebarkan (CMRR) diperbuat daripada InGaAsP / InP semikonduktor dibentangkan menggunakan graf aliran isyarat (SFG) kaedah yang membolehkan memodelkan fungsi pemindahan CMRR pasif. Penapis pasif ini kebanyakannya mempunyai ciri-ciri sambutan frekuensi mereka. Pengiraan secara teori sistem ini dilaksanakan oleh kesan analisis Vernier. Dua MRRs dengan radius 100 mikron yang menegak serta bersama-sama digunakan untuk menjana puncak salunan. Di sini, fasa , penyebaran dan kumpulan kelewatan isyarat yang dihasilkan dianalisis.

Kata kunci: Semikonduktor InGaAsP/InP, penyebar resonator mikroring, kesan Vernier, fasa, penyebaran dan punyebaran kumpulan

1.0 INTRODUCTION

The microring resonator (MRR) use light and follow the principles behind constructive interference and total internal reflection [1]. When light of the resonant wavelength is passed through the system from the input port, it builds up in intensity over multiple round-trips due to constructive interference and is output to the output port which serves as a detector waveguide [2]. The optical MRR functions as a filter because only a select few wavelengths will be at resonance within the loop [3]. The MRR can be integrated with two or more ring waveguides to form an add-drop filter system [4]. Optical filters are designed based on electromagnetic models to solve the fields in the frequency/wavelength or time domain [5]. Optical filter is generally acted as an interferometer which cleaves the input signal into several paths with delaying, recombining and wavelength independent approach [6, 7]. The variation in splitting and recombining ratios and delays leads to change in the frequency response [8]. These filters are mostly characterized by their frequency response [9]. In the context of signal processing, several analytical methods, such as the scattering matrix method and the transfer-matrix-chain-matrix algebraic method have been introduced to determine optical filter transfer functions in the Z-domain [10]. The Vernier operation with signal flow graph (SFG) method is a graphical approach [11] for analyzing the intricate photonic circuits and quick calculation of optical transfer function [12]. The SFG technique has some distinct advantages such as the graphical representation of signals behavior with the optical system. It is able to provide simple and a systematic technique of controlling the system's variables.

2.0 THEORETICAL BACKGROUND

The mathematics solution of the MRR system is based on the Vernier effect calculations for the CMRR. A resonating layout including a double stage MRR with 2 × 2 optical couplers which are vertically coupled together is shown in Figure 1(a). The signal flow graph (SFG) diagram of 2 × 2 optical directional couplers is displayed in Figure1 (b). By taking into account the insertion loss γ and the coupling factor k_i of the i^{th} coupler (i=1,2,3 for each coupler), the fraction of light pass through the throughput path is expressed as $C_i = \sqrt{(1-\gamma_i)(1-k_i)}$ and in contrast, the fraction of light pass through the cross path is expressed as $S_i = \sqrt{(1-\gamma_i)k_i}$. The Z-transform parameter is defined as $Z^{-1} = \exp(-j\,2\pi\, n_{eff}\, L/\lambda)$, where n_{eff} is the effective refractive index of the waveguide, λ is the center wavelength and the circumference of the ring is $L = 2\pi R$, here R represents the radius of the MRR. Based on the Mason's rule the optical transfer function, H, for an optical device with the input photonics node $E_i(z)$ and the output photonics node $E_n(z)$ is

$$H = \frac{E_n(z)}{E_i(z)} = \frac{1}{\Delta}\sum_{j=1}^{n} T_j\,\Delta_j \qquad (1)$$

where T_j shows the gain of the i^{th} forward path from the input to output port and n is the overall number of onward paths from input to output photonics nodes. The symbol Δ_j considers all of the loops that remain untouched while a signal transverses via each T_j forward path from input to output photonics nodes. The signal flow graph determinant is displayed by Δ, which is given by

$$\Delta = 1 - \sum_{i=1} L_i + \sum_{i\neq j} L_i\, L_i - \sum_{i\neq j\neq k} L_i\, L_j L_k + \ldots \qquad (2)$$

Here L_i is the transmittance gain of the i^{th} loop. The SFG for our proposed system is illustrated in Figure 1(b), in which the input node is $E_1=E_{in}$ and $E_{12}=E_{drop}$ are considered as the drop node. The Free Spectral Range (FSR) of the device is determined by $FSR = c/n_g\, L$ where $n_g = n_{eff} + f_0(dn_{eff}/df)_{f_0}$ is the group refractive index of the ring, n_{eff} is the effective refractive index, and f_0 is the design (center) frequency [13]. The FSR of the CMRR with different radii can be determined by [14]

$$FSR_{tot} = N_1.FSR_1 = N_2.FSR_2 \qquad (3)$$

where N_1 and N_2 are integer resonant mode numbers of each rings which can be determined by the ratio of FSR_{tot} rather than the FSR of each rings (FSR_i). To determine the optical transfer function (OTF), non-touching loops and forward transmittance paths have to be identified from SFG diagram. The CMRR system is shown in Figure 1.

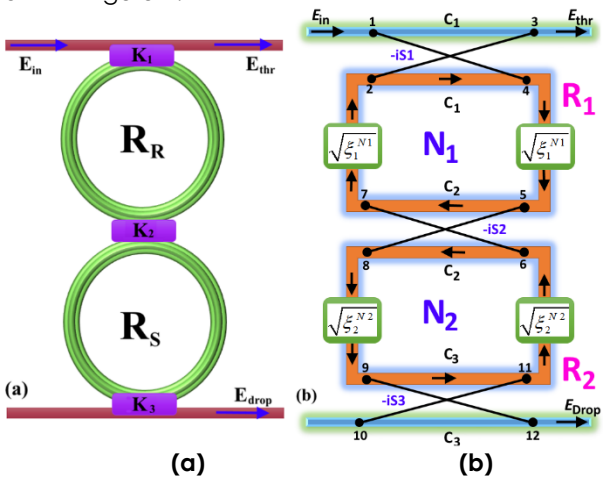

Figure 1 CMRR configuration (a) waveguide layout and (b) Z-transform diagram SFG

From Figure 1(b), three individual loops can be found for the CMRR as equation 4. Two separate and non-touching transmittance loops from L_1 and L_2 exist as equation 5. Three onward route transmittances with their delta determinant, Δ_i, recognizes from input node 1 to through node 3. The first transmittance onward path belongs to direct route which pass via (1→3) photonics nodes is given by equation 6. The four non-touching loops also can be considered for this path so the delta determinant for this rout is given by equation 7.

The second route goes to the track passes via these photonics nodes (1→4→5→7→2→3). Hence, the second transmittance path is expressed by equation 8. For this track only one non-touching loop, L_2, can be found which make the delta determinant as shown by equation 9. The third transmittance route is the track which traverses via both rings through (1→4→5→8→9→11→6→7→2→3) photonics nodes shown by equation 10. There is not any non-touching loop for this track so the delta determinant can be expressed by equation 11. Considering coupling loss $C_i^2 + S_i^2 = 1 - \gamma_i$ in addition to use the Mason rule for CMRR filter from the Equation (1), the OTF for throughput port of CMRR Vernier filter can be calculated as by equation 12. The same procedure can be done for drop port of the CMRR but transmittance forward paths changes to a track passes from (1→4→5→8→9→12) nodes.

The drop port transmittance path changes to equation 13. Since this path touches all loops, the delta determinant for this path is equal to one shown by equation 14. Employing Mason's rule for drop port, the OTF for drop port CMRR Vernier filter is expressed by equation 15.

$$L_1 = C_1 C_2\ \xi_1^{N1},\ L_2 = C_2 C_3\ \xi_2^{N2},\ L_3 = -C_1 C_3\ S_2^2\ \xi_1^{N1}\xi_2^{N2} \quad (4)$$

$$L_4 = L_1 . L_2 = C_1 C_2^2\ C_3\ \xi_1^{N1}\ \xi_2^{N2} \quad (5)$$

$$T_1^{thr} = C_1 \quad (6)$$

$$\Delta_1^{thr} = 1 - (L_1 + L_2 + L_3) + L_4 \quad (7)$$

$$T_2^{thr} = -\ S_1^2\ C_2\ \xi_1^{N1} \quad (8)$$

$$\Delta_2^{thr} = 1 - L_2 = 1 - C_2 C_3\ \xi_2^{N2} \quad (9)$$

$$T_3^{thr} = S_1^2\ S_2^2\ C_3\ \xi_1^{N1}\xi_2^{N2} \quad (10)$$

$$\Delta_3^{thr} = 1 \quad (11)$$

$$H_{31}^{thr} = \frac{\{C_1 - (1-\gamma_1)C_2\ \xi_1^{N1} - C_1 C_2 C_3\ \xi_2^{N2} + (1-\gamma_1)(1-\gamma_2)C_3\ \xi_1^{N1}\xi_2^{N2}\}}{\{1 - C_1 C_2\ \xi_1^{N1} - C_2 C_3\ \xi_2^{N2} + (1-\gamma_2)C_1 C_3\ \xi_1^{N1}\ \xi_2^{N2}\}} \quad (12)$$

$$T_1^{drp} = -i\ S_1 S_2\ S_3 \sqrt{\xi_1^{N1}}\sqrt{\xi_2^{N2}} \quad (13)$$

$$\Delta_1^{drp} = 1 \quad (14)$$

$$H_{31}^{thr} = \frac{-i\ S_1 S_2\ S_3 \sqrt{\xi_1^{N1}}\sqrt{\xi_2^{N2}}}{\{1 - C_1 C_2\ \xi_1^{N1} - C_2 C_3\ \xi_2^{N2} + (1-\gamma_2)C_1 C_3\ \xi_1^{N1}\ \xi_2^{N2}\}} \quad (15)$$

To obtain optimum coupling for higher transmission in drop port, we supposed that the input signal is totally coupled into the ring resonator and the transmission in through port is zero, $H_{82}^{thr} = 0$ [15]. For further simplification with considering the exponential series up to the 1st order we suppose $\xi_1^{N1} = \xi_2^{N2} \approx 1$ as the imaginary part will vanish in resonance condition. For a choice of $k_2 = k_3$ the value of k_1 is determined as [16]

$$k_1 = 1 - \frac{(1-\gamma_2)(1-\gamma_1)(1-k_2)[1-(1-\gamma_2)]^2}{[1-(1-k_2)(1-\gamma_2)]^2} \quad (16)$$

where γ_i represent the intensity insertion loss coefficients for couplers between rings and the bus waveguides [4, 17].

3.0 RESULTS AND DISCUSSION

Two MRRs with radius of 100 µm which are vertically coupled together are used to generate resonant peaks as shown in Figure 2(a). The resonating system are fabricated from III/V semiconductors (InGaAsP/InP) on the basis of InP with a direct bandgap [18]. The propagation loss is 0.1 dB/cm and the waveguide cores are 0.25 µm^2. Based on equation 1, the resonant mode numbers for this optical system get equal values since the material and the length of both rings are the same. The waveguide's intensity attenuation coefficient is $\alpha = 0.1 dB/cm$ [19, 20], intensity insertion loss coefficients for couplers between rings and the bus waveguides are $\gamma_1 = 0.0001$ and $\gamma_2 = \gamma_3 = 0.001$. An often-used component in microring-based optical circuitry is the directional coupler-a twin waveguide structure used to couple a fraction of light from one waveguide to another [21]. Directional couplers are used to transfer light into and out of a MRR, and can be designed with a high degree of accuracy [22]. The coupling coefficients are selected to $\kappa_1 = \kappa_2 = \kappa_3 = 0.02$. The input laser power versus the wavelength variations is shown in Figure 2.

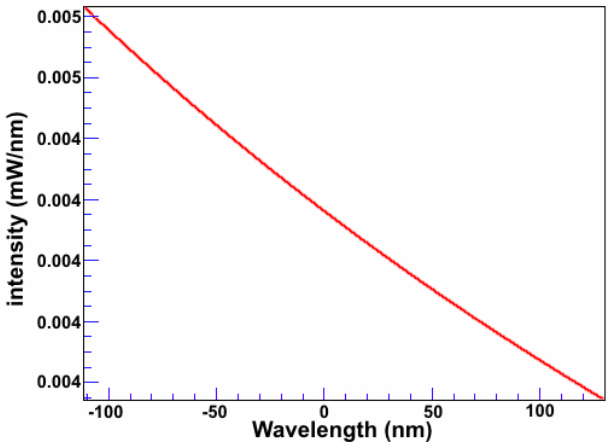

Figure 2 Input power versus the wavelength variation

As the resonators are weakly coupled, an optical signal in the structure effectively takes a longer time to tunnel from resonator to resonator. We coupled light into the device by butt coupling a single-mode fiber to the facet. Figure 3(a-b) shows the through port phase response versus the wavelength and frequency respectively.

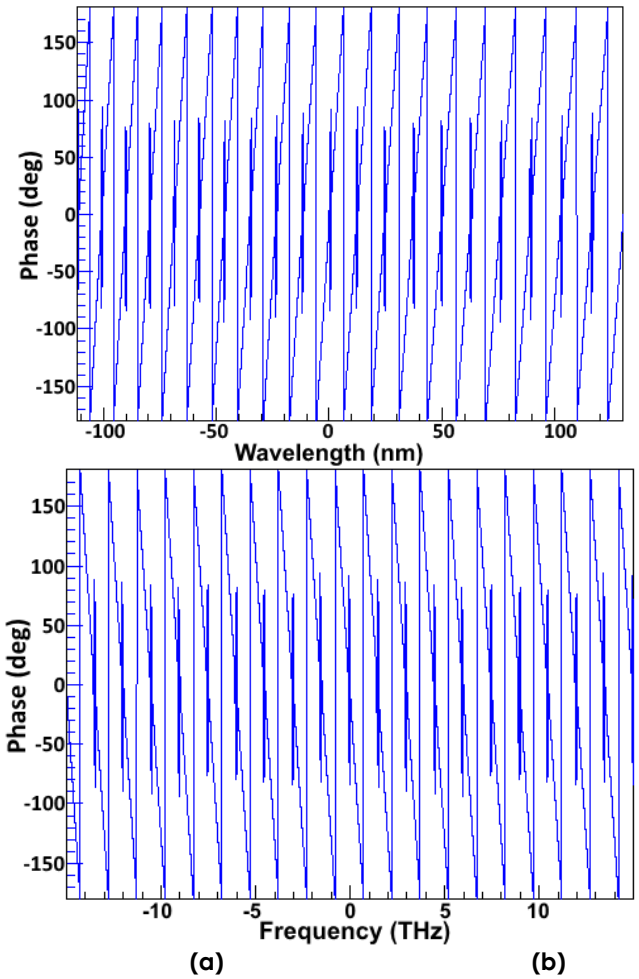

Figure 3 Through port phase response, (a): Phase response versus wavelength, (b): Phase response versus frequency

Figure 4(a-b) shows the drop port phase response versus the wavelength and frequency respectively.

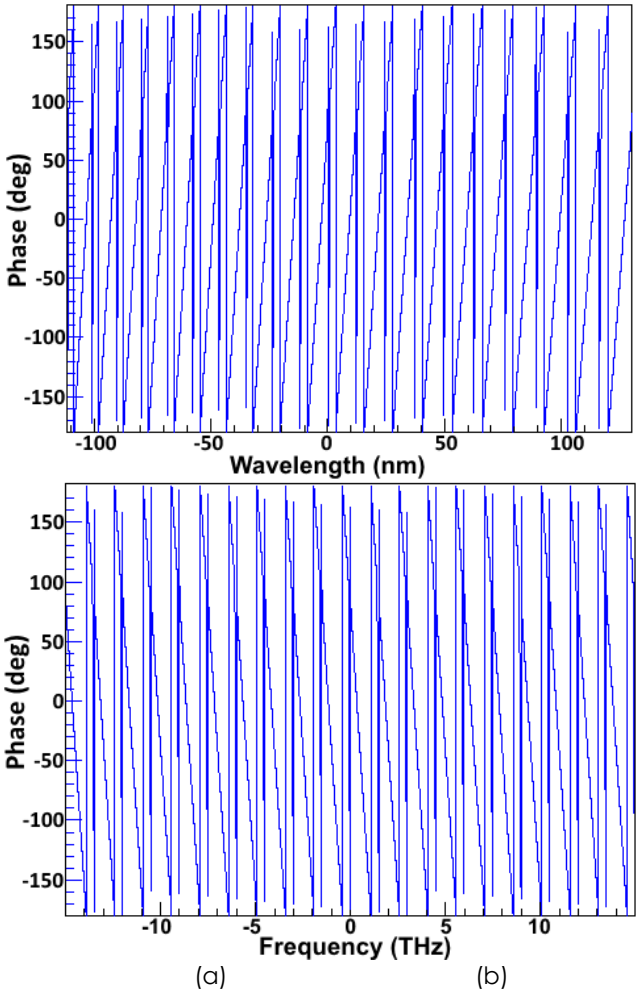

Figure 4 (a): Drop port phase response, (a): Phase response versus wavelength, (b): Phase response versus frequency

Dispersion measures the rate of change of the group delay regarding to the wavelength. Several factors contributors to dispersion [23, 24]. There is waveguide dispersion due to the fact that the electromagnetic wave is constrained to propagate in a guide of a given shape and cross sectional area. There is material dispersion due to the fact that the refractive indices involved are wavelength dependent. There is intermodal dispersion caused by the mixing of modes in a multi-mode system that is of no concern under single-mode operation [25]. Finally there is structural dispersion that is determined by the architecture of the filter. The dispersion responses of the through port of the CMRR is shown in Figure 5.

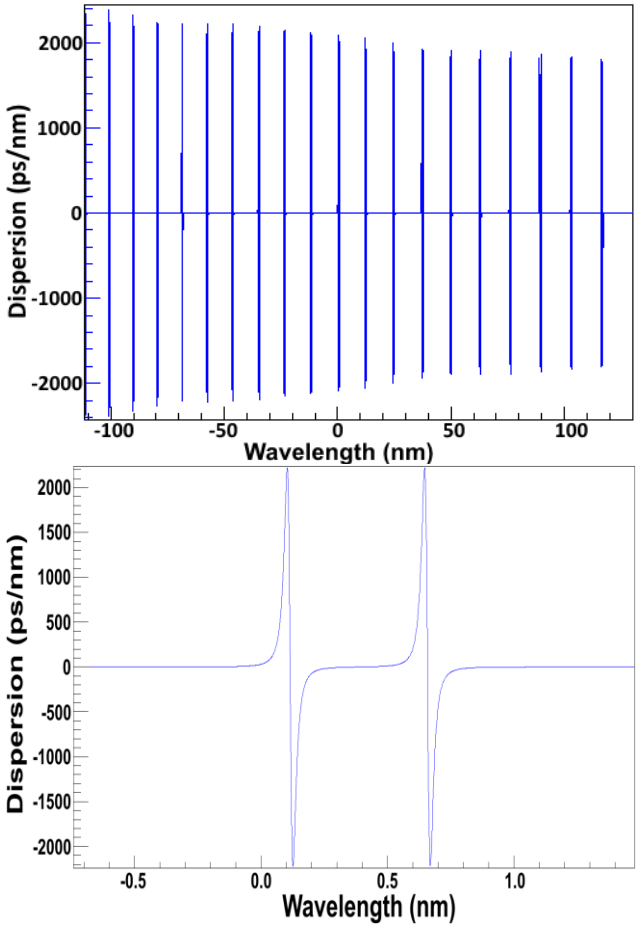

Figure 5 Through port dispersion response reference to the input port versus wavelength

The dispersion response of the through port reference to the drop port of the CMRR is shown in Figure 6.

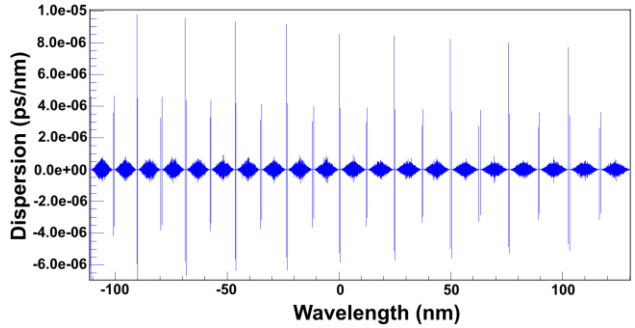

Figure 6 Through port dispersion response reference to the drop port versus wavelength

Figure 7 shows the dispersion responses of the drop port reference to the input port of the CMRR.

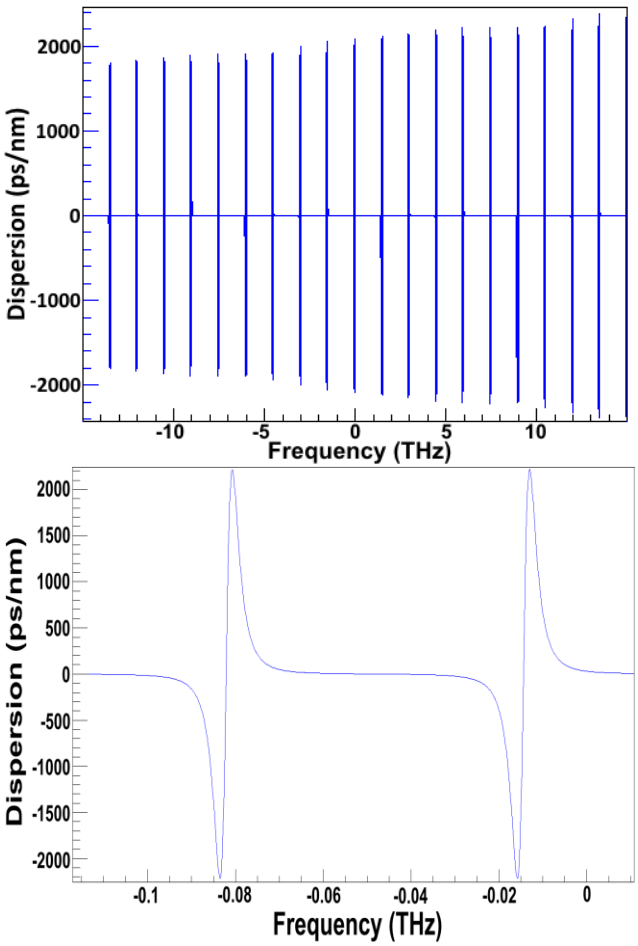

Figure 7 Drop port dispersion response reference to the input port versus frequency

Figure 8(a-b) shows the group delay of the drop port reference to the input port versus wavelength and frequency respectively, where Figure 9 shows the group delay reference to the through port versus wavelength and frequency respectively.

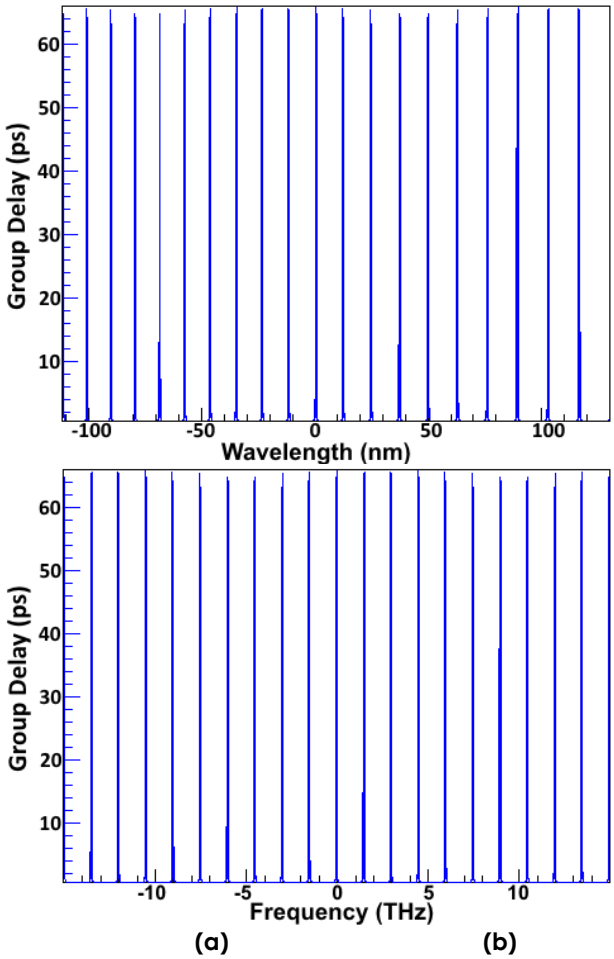

Figure 8 (a): Group delay (ps) of the drop port reference to the input port versus wavelength, (b): Group delay (ps) versus frequency

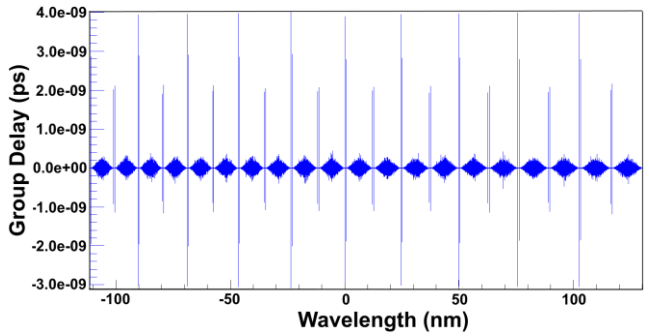

Figure 9 Group delay (ps) of the drop port reference to the through port versus wavelength

The performance of the passive ring resonators for filter application is limited by the internal losses. The incorporating of a semiconductor optical fiber (SOA) enables additional functionality such as the compensation of internal losses. Thus, the combination of a passive and active material enables the possibility to realize ring resonators with integrated SOA similar to the fiber optic filters with erbium-doped fiber amplifiers (EDFA), for improved filter performance of multi coupled ring resonator devices.

4.0 CONCLUSION

A cascaded microring resonator (CMRR) is presented to show and analyze the phase, dispersion and group delay responses. This system consists of two MRRs vertically coupled which have the same radius. The input laser pulse is used to propagate within the MRR system. This system act as add/drop MRR system so that the spectrum of the input pulse will experiences the constructive and destructive interferences. The mathematics solution of the system is performed using the Vernier effect, where the signal flow graph (SFG) is used to analyze the complex photonic circuits mathematically.

Acknowledgement

The author IS Amiri would like to acknowledge the University Malaya/MOHE under grant number UM.C/625/1/HIR/MOHE/SCI/29, LRGS (2015) NGOD/UM/KPT and RU 007/2015 from the University of Malaya (UM). The author SE Alavi would like to acknowledge the grant number Q.J130000.2609.10J97 from the Universiti Teknologi Malaysia (UTM).

References

[1] Amiri, I., Soltanian, M., Alavi, S., Othman, A., Razak, M. And Ahmad, H. 2015. Microring Resonator For Transmission Of Solitons Via Wired/Wireless Optical Communication. *Journal of Optics*.

[2] Afroozeh, A., Amiri, I. S., Farhang, Y. And Zeinalinezhad, A. 2015. Microring Resonators: Fabrication and Applications in Soliton Communications. Amazon.

[3] Amiri, I. S., Alavi, S. and Ahmad, H. 2015. Increasing Access Points in a Passive Optical Network. *Optics and Photonics News*.

[4] Amiri, I. S., Alavi, S., Soltanian, M., Penny, R., Supa'at, A. and Fisal, N. 2015. 2×2 MIMO-OFDM-Rof Generation and Transmission of Double V-Band Signals using Microring Resonator System. *Optical and Quantum Electronics*.

[5] Amiri, I. S., Alavi, S. and Ahmad, H. 2015. Microring Resonators used to Gain the Capacity in a High Performance Hybrid Wavelength Division Multiplexing System. *In Horizons In World Physics.* 287.

[6] Soltanian, M., Ahmad, H., Khodaie, A., Amiri, I. S., Ismail, M. F. and Harun, S. W. 2015. A Stable Dual-Wavelength Thulium-Doped Fiber Laser at 1.9 μm using Photonic Crystal Fiber. *Scientific Reports*.

[7] Soltanian, M., Amiri, I. S., Alavi, S. and Ahmad, H. 2015. Dual-Wavelength Erbium-Doped Fiber Laserto Generate Terahertz Radiation using Photonic Crystal Fiber. *Journal of Lightwave Technology*.

[8] Amiri, I. S., Alavi, S. and Ahmad, H. 2015. Fiber Laser Setup Used to Generate Several Mode-Locked Pulses Applied to Soliton-Based Optical Transmission Link. *In Horizons In World Physics.* 287.

[9] Amiri, I. S. and Ahmad, H. 2015. Optical Soliton Signals Propagation in Fiber Waveguides. Ed Springer. 1-11.
[10] Soltanian, M., Amiri, I., Chong, W., Alavi, S. and Ahmad, H. 2015. Stable Dual-Wavelength Coherent Source with Tunable Wavelength Spacing Generated by Spectral Slicing a Mode-Locked Laser using Microring Resonator. *IEEE Photonics Journal*. 7.
[11] Bahadoran, M., Ali, J. and Yupapin, P. P. 2013. Graphical Approach for Nonlinear Optical Switching by PANDA Vernier Filter. *IEEE Photonics Technology Letters*. 25: 1470-1473.
[12] Amiri, I. S. 2015. Soliton-Based Microring Resonators: Generation and Application in Optical Communication. Amazon.
[13] Sirawattananon, C., Bahadoran, M., Ali, J., Mitatha, S. and Yupapin, P. P. 2012. Analytical Vernier Effects of a PANDA Ring Resonator for Microforce Sensing Application. *IEEE Transactions on Nanotechnology*. 11: 707-712.
[14] Amiri, I. S. and Ahmad, H. 2015. Ultra-Short Solitonic Pulses Used in Optical Communication. Springer. 47-51.
[15] Amiri, I. S. and Ahmad, H. 2015. Solitonic Signals Generation and Transmission using MRR. *Ed:* Springer. 31-46.
[16] Amiri, I. S. and Afroozeh, A. 2015. Spatial and Temporal Soliton Pulse Generation by Transmission of Chaotic Signals using Fiber Optic Link. *Journal Of Optics Research*. 16.
[17] Afroozeh, A., Amiri, I. S., Chaudhary, K., Ali, J. and Yupapin, P. P. 2015. Analysis of Optical Ring Resonator. *Journal Of Optics Research*. 16.
[18] Amiri, I. S., Alavi, S. E. and Ahmad, H. 2015. Optically Generation and Transmission Ultra-Wideband Mode-Locked Lasers using Dual-Wavelength Fiber Laser and Microring Resonator System. *In Horizons in World Physics*. 287.
[19] Amiri, I. S., Soltanian, M. and Ahmad, H. 2015. Application of Microring Resonators (MRRS) in Optical Soliton Communications. Ed: Novascience Publisher.
[20] Amiri, I. S., Alavi, S. E., Soltanian, M. R. K., Fisal, N., Supa'at, A. S. M. and Ahmad, H. 2015. Increment of Access Points in Integrated System of Wavelength Division Multiplexed Passive Optical Network Radio Over Fiber. *Scientific Reports*. 5.
[21] Amiri, I. S., Alavi, S. E., Soltanian, M., Ahmad, H., Fisal, N. and Supa'at, A. 2015. Experimental Measurement of Fiber-Wireless Transmission via Multimode-Locked Solitons from a Ring Laser EDF Cavity. *IEEE Photonics Journal*. 7: 1-9.
[22] Amiri, I. S. and Ahmad, H. 2015. Microring Resonator (MRR) Optical Systems Applied to Enhance The Soliton Communications. Ed: Novascience Publisher.
[23] Amiri, I. S. and Ahmad, H. 2015. MRR Systems and Soliton Communication. *Ed: Springer.* 13-30.
[24] Amiri, I. S. 2014. Optical Soliton Based Communication using Ring Resonators. Universiti Teknologi Malaysia, Faculty Of Science.
[25] Ahmad, H., Soltanian, M., Amiri, I. S., Alavi, S. E. and Othman, A. 2015. Carriers Generated by Mode-Locked Laser to Increase Serviceable Channels in Radio Over Free Space Optical Systems. *IEEE Photonics Journal*. 7.